ISBN: 978-3-95450-261-5 ISSN: 2673-7000 doi: 10.18429/JACoW-NAPAC2025-WEP091

TRANSVERSE DEFLECTING CAVITY OPTIMIZATION FOR ACTIVE CONTROL OF ELECTRON BEAM ENERGY CHIRP*

H. Xu†, Q. Marksteiner, N. Yampolsky
Los Alamos National Laboratory, Los Alamos, USA
G. Chen, A. DeSimone[1], S. Doran, G. Ha[1], W. Liu, R. Margraf-O'Neal, J. Power, E. Wisniewski[1]
Argonne National Laboratory, Lemont, USA
[1]also at Northern Illinois University, DeKalb, USA

Abstract

The Transverse Deflecting Cavity Based Chirper (TCBC) is a novel concept of imposing and removing a significant energy chirp of an ultrarelativistic electron beam. The TCBC method requires much less footprint, compared to the conventional chirping and dechirping method involving operating a linear accelerator off-crest. When the compressed bunch is very short, the dechirping has to rely on the wakefields. We present our updated design of the L-band (1.3 GHz) transverse deflecting cavity (TDC) for demonstrating the TCBC concept at the Argonne Wakefield Accelerator (AWA) Facility. Our TDC design update is based on the original design provided by Tsinghua University. The TDC design update focused on ensuring improved performance under more intense electromagnetic fields, reducing the peak pulsed temperature rise. The tuners of the TDC were meanwhile reworked to allow greater adjustability of the resonant frequency and of the electromagnetic field balance among the cells. We also report the tolerance study of the TDC. Two copies of the TDC with the updated design are currently under fabrication with Dymenso, LLC.

INTRODUCTION

At Los Alamos National Laboratory (LANL), a novel approach of creating and removing the energy chirp in an ultrarelativistic electron beam is under investigation, namely the Transverse Deflecting Cavity Based Chirper (TCBC) method [1]. The conventional method of imposing and eliminating the energy chirp involves accelerating the electron beam off the RF phase crest, leading to inefficient utilization of the available space and longer linear accelerator (linac) sections. In comparison, the TCBC brings about a better optimized tradeoff of beamline arrangement: a dedicated TCBC beamline is inserted for imposing and eliminating the energy chirp, but the benefit is that all linac modules can operate at an RF phase optimized solely for the purpose of beam acceleration, leading to a net reduction of beamline length and thus cost.

The key element of the TCBC beamline is the radiofrequency (RF) transverse deflecting cavities (TDC). A typical TCBC beamline involves three TDCs. The first TDC creates a linear transverse momentum kick long the beam; the head and tail of the beam are kicked in opposite directions, with the center of the beam unperturbed. The second TDC imprints a linear energy difference according to the transverse position of the beam particles, creating or eliminating the energy chirp. The third TDC resets the transverse momentum distribution initially created by the first TDC. Quadrupoles are involved between neighboring TDCs for precise control of the transverse phase spaces of the beam.

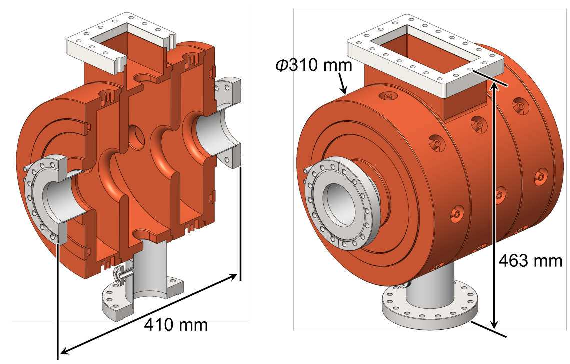

Figure 1: Half section view and external view of the 1.3-GHz TDC model in SolidWorks.

A LANL-AWA collaboration has been established for experimentally demonstrating the TCBC concept at AWA with a 40-MeV electron bunch [2]. The preliminary beamline configuration has been determined, and refined beamline modeling is ongoing.

In this paper, we report the design upgrade of the 1.3-GHz TDCs currently in operation at Argonne Wakefield Accelerator (AWA) Facility. The TDCs at AWA were initially designed and fabricated at Tsinghua University [3]. For the TCBC experimental study, LANL and AWA put an effort together to refine the TDC design, before the fabrication of two new copies of the TDC. The TDC, with refined features added, is shown in Fig. 1.

RF DESIGN REFINEMENT

The RF design refinement of the TDC included three revisions. First, we increased the fillet size of the RF coupling apertures between the coupling cells and the central cell, and of the input RF power coupling slot. Second, we adjusted the inner diameters of the three cells to ensure that when the TDC operates at the designed temperature, the resonant frequency shall be 1300.00 MHz. Third, we performed tol-

* Work supported by U.S. Department of Energy through the Laboratory Directed Research and Development program of Los Alamos National Laboratory, under project number 20240231ER.
† haoranxu@lanl.gov

ISBN: 978-3-95450-261-5 ISSN: 2673-7000 doi: 10.18429/JACoW-NAPAC2025-WEP091

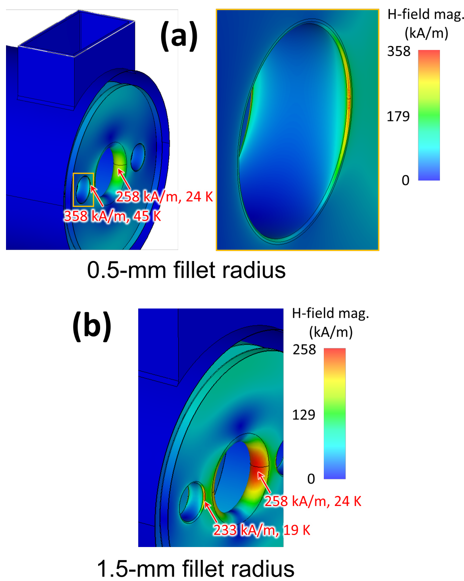

Figure 2: 1.3-GHz magnetic field magnitude distribution in the TDC, highlighting the peak magnetic field in (a) the original TDC design and (b) the updated design.

erance studies to update the requirements on the tolerances of critical dimensions of the cavity.

In the original design, as shown in Fig. 2a, the edges of the RF coupling apertures between the coupling cells and the central cell were designed to have a fillet size of 0.5 mm. When the TDC operates under an input RF power of 10.0 MW, the blended edges facing the central cell will witness a peak magnetic field of 358 kA/m at 1.3 GHz. With a pulse length of 10 µs, the pulsed temperature rise will be 45 K, which is at the threshold of causing cyclic fatigue if the cavity operates long term. Therefore, we increased the fillet size at these edges and at the RF coupling slot edges to 1.5 mm, and the abovementioned temperature rise was reduced to 19 K. Meanwhile, after this revision, the peak magnetic field location of the cavity is at the iris faces towards the central cell, where the temperature rise is 24 K.

We then targeted a room-temperature operating frequency of 1300.32 MHz of the TDC for the RF design refinement, so that when the cavity is heated up during operation, the operating frequency will be reduced to very close to 1300.00 MHz due to thermal expansion, fine-tuned by the cooling water temperature. The cavity RF performance was studied using the CST High Frequency Solver, and the normalized on-axis RF magnetic field distribution providing the beam deflection is shown in Fig. 3.

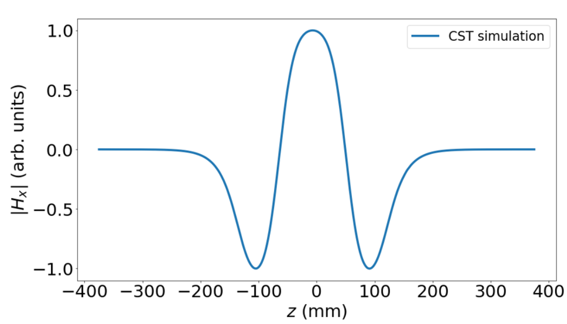

Figure 3: 1.3-GHz TDC on-axis distribution of the magnetic field providing beam deflection.

The tolerances of selected critical dimensions (Fig. 4) were evaluated through CST simulations. Four sets of simulations were performed. In each set, the inner diameters of cells ($\Phi_{cpl,1}$, Φ_{ctl}, $\Phi_{cpl,2}$), central cell apertures ($\Phi_{a,1}$, $\Phi_{a,2}$), the depths of cells ($D_{cpl,1}$, D_{ctl}, $D_{cpl,2}$), and central cell iris thicknesses (d_1, d_2) were varied, respectively, while the other three groups of parameters were held as the design values. The tolerance specifications used in the fabrication and the resulting maximal shift ranges of the resonant frequency are listed in Table 1. It can be seen that the diameters had much more impact on the resonant frequency shifts, because each individual cell can be considered as operating in the zero mode in the longitudinal direction.

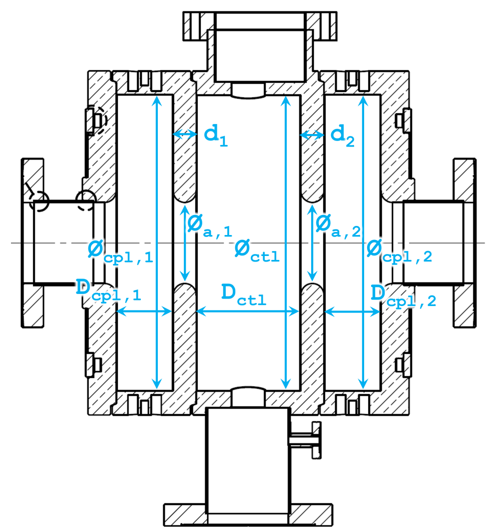

Figure 4: Selected critical dimensions used in the tolerance study of the 1.3-GHz TDC.

RF PROBE AND TUNING

The upgraded design also features the addition of a 50-Ω RF probe for sampling the magnitude of the RF field as a feedback for precise control of the input RF power. As shown in Fig. 5, the probe is located in the field cut-off region, and the transmission of RF from the input RF port to the probe is −59.6 dB. The probe was designed at AWA for the 1.3-GHz linac [4], and a half section view is provided in Fig. 6.

We increased the total number of the tuning divots to eight for the coupling cells, and to six for the central cell. Because the TDC operates in the TM11 mode, when the tuning studs are moved by a same amount, the frequency tuning provided by the tuning studs at different azimuthal positions will vary. According to the prior study at AWA, the safe limits of the physical displacement of the tuning studs using this design are ±0.063 inch [5], measured in the radial direction.

ISBN: 978-3-95450-261-5 ISSN: 2673-7000 doi: 10.18429/JACoW-NAPAC2025-WEP091

Table 1: Tolerances of Dimensions and Resulting Resonant Frequency Shifts

Dim.	**Val. (inch)**	**Max. Δf_0 (MHz)**
$\Phi_{cpl,1}$	10.514$\pm$0.001	
Φ_{ctl}	10.501$\pm$0.001	$\pm$0.126
$\Phi_{cpl,2}$	10.514$\pm$0.001	
$\Phi_{a,1}$	2.874 (0.000, +0.002)	(-0.042, 0.000)
$\Phi_{a,2}$	2.874 (0.000, +0.002)	
$D_{cpl,1}$	2.024$\pm$0.002	
D_{ctl}	3.714$\pm$0.002	$\pm$0.019
$D_{cpl,2}$	2.024$\pm$0.002	
d_1	0.822$\pm$0.002	$\pm$0.012
d_2	0.822$\pm$0.002	

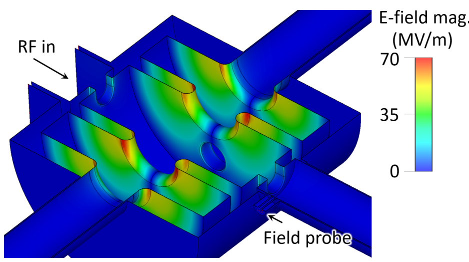

Figure 5: Half section view of the RF electric field magnitude distribution of the TDC with an input RF power of 10 MW. The positions of the input RF waveguide port and the RF probe are annotated.

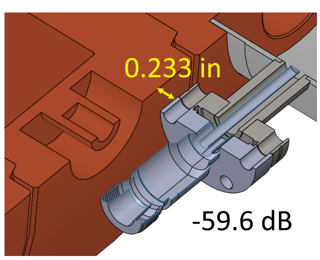

Figure 6: Half section view of the 50-Ω RF probe assembled on the TDC. The 30-mm diameter tuning divot is also shown.

The tuning of the TDC was studied in the CST High Frequency Solver. We studied two scenarios. First, if the field balance of the TDC is held constant at 1:1:1, then the maximal frequency tuning range will be $\pm$0.1MHz. Second, if we aim at the maximal frequency tuning range, disregarding the field balance, then the maximally achievable tuning range will be $\pm$0.5 MHz, and the resulting field balance will be $1.00 \pm 0.03 : 1.00 : 1.00 \pm 0.03$.

FABRICATION

The brazing joints between the longitudinal copper sections of the TDC were redesigned, working with Dymenso, LLC, the manufacturer of the new TDCs. The brazing joints had an angle of 110 degrees, with a 0.001-inch gap reserved for the gold-copper braze washer sheet. On the atmosphere side of the brazing joint, a wider gap is used as brazing dam. Fig. 7 shows the precision-machined TDC parts under the brazing process. The brazing of copper parts to stainless steel components and the copper-copper brazing were performed separately.

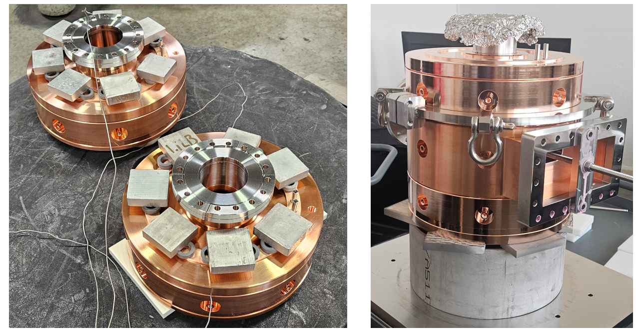

Figure 7: TDCs under fabrication at Dymenso, LLC.

CONCLUSIONS

A collaborated effort between Los Alamos National Laboratory and Argonne Wakefield Accelerator Facility is ongoing, for experimentally investigating the Transverse Deflecting Cavity Based Chirper concept, which is promising in reducing footprint and cost of future facility linear accelerators for applications such as free electron laser, where chirping and dechirping an electron beam is entailed.

In order to carry out the experiment at AWA, two new TDCs were fabricated with an upgraded design. The design upgrade was intended for improved TDC operating performance, including refinement of RF design, an RF probe, and redesigned tuning divot geometry.

REFERENCES

[1] N. Yampolsky *et al.*, "Imposing strong correlated energy spread on relativistic bunches with transverse deflecting cavities," *Phys. Rev. Accel. Beams*, vol. 5, no. 5, p. 054403. `doi:10.1103/PhysRevAccelBeams.23.054403`

[2] A. DeSimone *et al.*, "Effects of beam conditions on achieving compact longitudinal de-chirping Using transverse deflecting cavities," presented at 2025 North American Particle Accelerator Conference(NAPAC'25), Sacramento, USA, Aug. 2025, paper WECN02, this conference.

[3] J. Shi *et al.*, "A 3-cell deflecting RF cavity for emittance exchange experiment at ANL," *Nucl. Instrum. Methods Phys. Res. A*, vol. 598, no. 2, pp. 388-393, 2009. `doi:10.1016/j.nima.2008.09.046`

[4] M. Conde *et al.*, "Commissioning of a 1.3-GHz deflecting cavity for phase space exchange at the Argonne Wakefield Accelerator," in *Proc. IPAC'12*, New Orleans, USA, May 2012, pp.3350-3352. `https://jacow.org/IPAC2012/papers/THPPC031.pdf`

[5] J.G. Power *et al.*, "Tuning, conditioning, and dark current measurements: 1300 MHz NCRF cavities at the Argonne Wakefield Accelerator (AWA) Facility," in *Proc. PAC2013*, Pasadena, USA, Sep 2013, pp. 996-998. `https://jacow.org/PAC2013/papers/WEPMA08.pdf`